J. Chem. Eng. Data **2005,** *50,* 1419−1424

Excess Molar Enthalpies of the Binary Carbon Dioxide + Dimethyl Carbonate System at Temperatures of (298.15 to 308.15) K and Pressures of (5.0 to 7.5) MPa

Hiroyuki Matsuda, Shigetaka Yoshii, Akinori Nagashima, Kiyofumi Kurihara, and Kenji Ochi*

Department of Materials and Applied Chemistry, Nihon University, 1-8 Kanda Surugadai,
Chiyoda-ku, Tokyo 101-8308, Japan

The excess molar enthalpies of the carbon dioxide + dimethyl carbonate system were measured in the vicinity of the critical point of carbon dioxide using a flow-type isothermal microcalorimeter at temperatures of (298.15 to 308.15) K and pressures of (5.0 to 7.5) MPa. Mixtures showed strong exothermic behavior in these regions. In addition, a strong pressure dependency of the excess molar enthalpies was observed, and the excess molar enthalpy values decreased with increasing pressure. The experimental results were correlated using a composition-dependent equation and the Peng−Robinson equation of state with van der Waals one-fluid mixing rules.

Introduction

Recently, rapid progress has been made in some studies on environmentally benign processes using supercritical fluids. In particular, the large heat effect of a mixture containing supercritical carbon dioxide (CO_2) is expected to be applied to new energy cycle systems, such as heat pumps. In the development of these energy-saving processes, the excess molar enthalpy (H^E) data in the vicinity of the critical point of CO_2 and in the supercritical region are important. Many researchers have studied these H^E data, especially Christensen et al., who have made detailed measurements of binary mixtures containing supercritical CO_2.[1−4] Previously, our group also measured four binary CO_2 and alcohol systems (methanol,[5−6] 2-propanol,[7] 2-butanol,[7] and 2-methyl-1-propanol[8]) and the ternary CO_2 + ethanol + water system,[8] and we found that the H^E data near the critical point of CO_2 often shows a large deviation in comparison to its behavior at low pressure, exhibiting a dramatic change in H^E with a small change in pressure.

In this study, we investigated dimethyl carbonate (DMC) as the second component for mixing with CO_2. DMC is a nontoxic substance that is widely used as a replacement for dimethyl sulfate, methyl halide, and phosgene in methylation and carbonylation reactions because it is considered to be an “environmentally benign building block”.[9−11] Therefore, if DMC is selected as the solvent for combining with supercritical CO_2 and if a large amount of heat is evolved, then this would be expected to be a very attractive option in the development of a heat cycle system. In addition, a new direct synthesis of DMC starting from CO_2 has been proposed by many research groups.[12−15] This method is attractive from an environmental point of view because it uses only CO_2 and methanol as raw materials and produces DMC and water, unlike other synthesis methods that use or produce toxic chemicals. Information on the thermodynamic properties of systems containing CO_2 and DMC is essential in the design and development of reaction and separation processes using these systems. Several authors have reported vapor−liquid equilibrium (VLE) data for the CO_2 + DMC system.[16,17] However, H^E data for this mixture are not available.

Thus, in this study, we have made detailed measurements of the H^E data for the CO_2 + DMC system at temperatures from (298.15 to 308.15) K and pressures from (5.0 to 7.5) MPa using a flow isothermal microcalorimeter. The experimental H^E data were correlated by the polynomial expression model and the Peng−Robinson (PR) equation of state (EOS) coupled with the van der Waals one-fluid mixing rule.

Experimental Section

Apparatus and Procedure. A high-pressure flow-type isothermal microcalorimeter (Calorimetry Sciences Corporation) was used to measure H^E. It consists of a mixing unit, a constant-temperature water bath, two high-pressure ISCO syringe pumps for sample supply, a cooling circulation system for the syringe, a pressure adjustment device, a degassing unit, and a personal computer for signal collection and data processing. Measurements can be made from (233 to 353) K and from (0.1 to 20) MPa. Details of the experimental apparatus and procedure have been described elsewhere.[5−8,18] In this study, a modified model of the mixing cell as described in the previous paper by Nagashima et al. was used.[18] In the improved mixing cell, both a mixing wire and concentric tubes were used to enhance the mixing of various systems. Degassing of liquids was carried out by combining a vacuum line and an ultrasonic wave unit. The temperature stability of the water bath is within ±0.0005 K. The reproducibility of our measurements can be estimated to be within ±1.0% (maximum absolute error is 8 $J\cdot mol^{-1}$), the uncertainty being due primarily to the high sensitivity of H^E values to small changes in temperature and pressure. In this study, the total flow rate was changed in the range of (0.05 to 0.20) $cm^3\cdot min^{-1}$, and the dependence of the total flow rate for the measurement of H^E was considered. The optimum total flow rate was 0.10 $cm^3\cdot min^{-1}$ for all cases studied.

---

* To whom correspondence should be addressed. E-mail: ochi@chem.cst.nihon-u.ac.jp. Phone: +81-3-3259-0793. Fax: +81-3-3293-7572.

10.1021/je050089u CCC: $30.25

Table 1. Densities ρ at T = 283.15 K of the Pure Components

	ρ/g·cm^{-3}	
P/MPa	CO$_2$^{a}	DMC^b
5.0	0.86863	1.08755
5.5	0.87548	1.08797
6.0	0.88178	1.08838
6.5	0.88763	1.08880
7.0	0.89311	1.08921
7.5	0.90313	1.08962

[a] NIST.[19] [b] Lugo et al.[20]

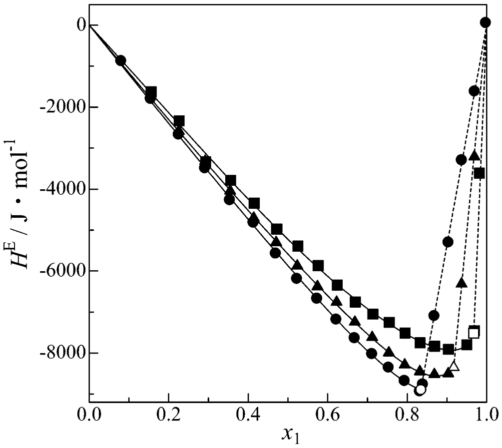

Figure 1. Experimental excess molar enthalpies for the system CO$_2$ (1) + DMC (2) at 298.15 K. This work: ●, 5.0 MPa; ▲, 5.5 MPa; ■, 6.0 MPa; −, eq 1; - - -, eq 5. Calculated solubility limit points: ○, 5.0 MPa; △, 5.5 MPa; □, 6.0 MPa.

For our measurements, the ISCO syringe was charged with each pure component after degassing. The temperatures of the syringes and their contents were kept constant in a water thermostat. In this study, a supply of pure components was kept at 283.15 K, which is about 20 K lower than the critical temperature of CO$_2$, to prevent variations in the density resulting from slight changes in the temperature and pressure. The pure components were then delivered to the mixing cell. The pumping rates of the liquids were calibrated by weighing the liquids delivered as a function of time.

Materials. The DMC used in this study was first grade pure reagent (Wako Pure Chemical Industry, Ltd., Japan) and was used after removing trace water with molecular sieves. The mole purity of DMC was checked by gas chromatography and was found to be above 99.9%. The volume fraction purity of the CO$_2$ was 99.99% (Showa Carbonic Acid Company, Ltd., Japan). Prior to use, the CO$_2$ was filtered through a 0.5 μm in-line filter (NUPRO Company).

Flow rates measured in cubic centimeters per minute at a constant temperature of 283.15 K were converted to moles per minute and to mole fractions using the densities of the pure materials, which were estimated as follows. The densities of CO$_2$ at 283.15 K and the pressures studied were cited from literature values.[19] The densities of DMC at 283.15 K and the pressures studied were obtained by interpolating the literature values of Lugo et al.[20] The calculated densities of the pure components are given in Table 1.

Results and Discussion

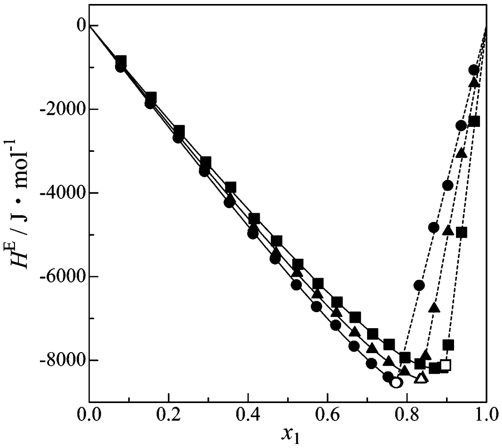

Figure 2. Experimental excess molar enthalpies for the system CO$_2$ (1) + DMC (2) at 303.15 K. This work: ●, 5.0 MPa; ▲, 5.5 MPa; ■, 6.0 MPa; −, eq 1; - - -, eq 5. Calculated solubility limit points: ○, 5.0 MPa; △, 5.5 MPa; □, 6.0 MPa.

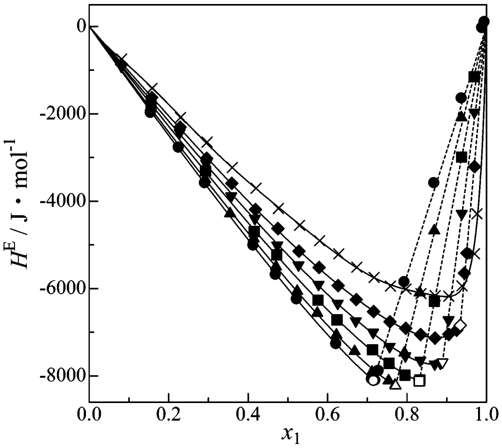

Figure 3. Experimental excess molar enthalpies for the system CO$_2$ (1) + DMC (2) at 308.15 K. This work: ●, 5.0 MPa; ▲, 5.5 MPa; ■, 6.0 MPa; ▼, 6.5 MPa; ◆, 7.0 MPa; ×, 7.5 MPa; −, eq 1; - - -, eq 5. Calculated solubility limit points: ○, 5.0 MPa; △, 5.5 MPa; □, 6.0 MPa; ▽, 6.5 MPa; ◇, 7.0 MPa.

H^E values were determined for the CO$_2$ + DMC system over the entire composition range at temperatures from (298.15 to 308.15) K under pressures from (5.0 to 7.5) MPa. The experimental results are listed in Table 2. Figures 1−3 show the plots of H^E against liquid mole fraction of CO$_2$ for the isobars studied at (298.15, 303.15, and 308.15) K, respectively. Mixtures in the region studied show large negative values of H^E. However, at 5.0 MPa and temperatures of (298.15 and 308.15) K, mixtures show slight endothermic mixing in the extremely CO$_2$-rich region. At each temperature and pressure, the mole fraction of CO$_2$ at which the maximum negative value appears shifts to the CO$_2$-rich side with an increase in the pressure. The largest negative value of H^E found in this study was about 8.9 kJ·mol^{-1} at 298.15 K and 5.0 MPa. At all temperatures and pressures except 308.15 K and 7.5 MPa, the H^E values vary linearly with the composition in the CO$_2$-rich region, which corresponds to the two-phase region.

Data Reduction

In this work, the experimental results for H^E in the homogeneous phase were correlated using the following polynomial expression model for the composition

$$H^E/\text{J}\cdot\text{mol}^{-1} = x_1(1 - x_1)\sum_{i=0}^{N-1}\frac{a_i(2x_1 - 1)^i}{\{1 - k(2x_1 - 1)\}} \qquad (1)$$

Table 2. Experimental Excess Molar Enthalpies for the System CO_2 (1) + DMC (2) at Different Temperatures

x_1^a	H^E/J·mol^{-1}	x_1^a	H^E/J·mol^{-1}	x_1^a	H^E/J·mol^{-1}	x_1^a	H^E/J·mol^{-1}	x_1^a	H^E/J·mol^{-1}	x_1^a	H^E/J·mol^{-1}
298.15 K, 5.0 MPa											
0.0793	−865	0.3528	−4257	0.5723	−6663	0.7523	−8345	0.8382^b	−8756	0.9364^b	−3285
0.1538	−1787	0.4121	−4806	0.6206	−7173	0.7924	−8669	0.8674^b	−7087	0.9688^b	−1605
0.2240	−2659	0.4683	−5560	0.6666	−7625	0.8307	−8924	0.9026^b	−5290	0.9969^b	64
0.2902	−3480	0.5216	−6179	0.7104	−8014						
298.15 K, 5.5 MPa											
0.1548	−1675	0.3546	−4045	0.5235	−5874	0.6682	−7244	0.7936	−8288	0.9033	−8502
0.2253	−2584	0.4139	−4706	0.5742	−6378	0.7120	−7618	0.8318	−8453	0.9368^b	−6314
0.2918	−3321	0.4702	−5301	0.6223	−6757	0.7537	−7993	0.8683	−8521	0.9691^b	−3208
298.15 K, 6.0 MPa											
0.1557	−1626	0.4156	−4343	0.5758	−5869	0.7134	−7051	0.8327	−7755	0.9502	−7801
0.2265	−2335	0.4718	−4974	0.6239	−6342	0.7550	−7255	0.8691	−7833	0.9693^b	−7458
0.2932	−3334	0.5252	−5395	0.6697	−6759	0.7947	−7515	0.9039	−7913	0.9817^b	−3615
0.3561	−3788										
303.15 K, 5.0 MPa											
0.0793	−992	0.3528	−4229	0.5723	−6715	0.7104	−8075	0.7766^b	−8530	0.9026^b	−3820
0.1538	−1865	0.4121	−4975	0.6206	−7161	0.7523	−8394	0.8307^b	−6211	0.9364^b	−2391
0.2240	−2683	0.4683	−5574	0.6666	−7663	0.7686	−8518	0.8674^b	−4826	0.9688^b	−1063
0.2902	−3485	0.5216	−6199								
303.15 K, 5.5 MPa											
0.0798	−896	0.3546	−4139	0.5742	−6431	0.7537	−8042	0.8392^b	−8422	0.9033^b	−4920
0.1548	−1834	0.4139	−4821	0.6223	−6870	0.7936	−8269	0.8466^b	−7900	0.9368^b	−3067
0.2253	−2591	0.4702	−5437	0.6682	−7338	0.8318	−8461	0.8683^b	−6765	0.9691^b	−1383
0.2918	−3339	0.5235	−5913	0.7120	−7732						
303.15 K, 6.0 MPa											
0.0803	−846	0.3561	−3861	0.5758	−6164	0.7550	−7622	0.8901	−8171	0.9372^b	−4940
0.1557	−1717	0.4156	−4615	0.6239	−6608	0.7947	−7934	0.8970^b	−8108	0.9693^b	−2289
0.2265	−2512	0.4718	−5147	0.6697	−6973	0.8327	−8087	0.9039^b	−7633		
0.2932	−3262	0.5252	−5706	0.7134	−7370	0.8691	−8190				
308.15 K, 5.0 MPa											
0.1537	−1967	0.4120	−5003	0.6205	−7259	0.7273^b	−7874	0.8674^b	−3575	0.9877^b	−22
0.2239	−2761	0.4682	−5674	0.7103	−8064	0.7923^b	−5842	0.9364^b	−1634	0.9939^b	112
0.2901	−3576	0.5215	−6236	0.7189^b	−8095						
308.15 K, 5.5 MPa											
0.1547	−1843	0.4138	−4856	0.5740	−6563	0.7119	−7909	0.7935^b	−7473	0.8682^b	−4675
0.2917	−3497	0.4700	−5497	0.6222	−7061	0.7536	−8107	0.8317^b	−6094	0.9368^b	−2083
0.3544	−4281	0.5234	−6060	0.6681	−7438	0.7698	−8208				
308.15 K, 6.0 MPa											
0.1556	−1782	0.6238	−6714	0.8690^b	−6291						
0.2931	−3307	0.7132	−7404	0.9372^b	−2992						
0.4154	−4696	0.7549	−7713	0.9692^b	−1153						
0.4717	−5228	0.7946	−7982								
0.5757	−6267	0.8326^b	−8094								
308.15 K, 6.5 MPa											
0.0807	−916	0.3574	−3884	0.5772	−5907	0.7145	−7004	0.8335	−7647	0.9044^b	−6718
0.1564	−1691	0.4169	−4398	0.6253	−6339	0.7560	−7329	0.8697	−7730	0.9376^b	−4285
0.2275	−2435	0.4733	−5011	0.6710	−6744	0.7956	−7544	0.8837	−7711	0.9694^b	−1967
0.2944	−3142	0.5266	−5463								
308.15 K, 7.0 MPa											
0.0812	−870	0.3587	−3592	0.5786	−5515	0.7571	−6760	0.8703	−7136	0.9443^b	−5649
0.1572	−1626	0.4184	−4190	0.6266	−5933	0.7966	−6911	0.9049	−7049	0.9507^b	−5190
0.2285	−2304	0.4747	−4626	0.6723	−6252	0.8343	−7053	0.9249	−6953	0.9697^b	−3208
0.2956	−3020	0.5280	−5143	0.7157	−6527						
308.15 K, 7.5 MPa											
0.0816	−744	0.3600	−3227	0.5799	−4905	0.7168	−5744	0.8350	−6117	0.9382	−5938
0.1579	−1415	0.4197	−3702	0.6279	−5205	0.7581	−5943	0.8710	−6161	0.9698	−5205
0.2294	−2087	0.4760	−4167	0.6734	−5509	0.7974	−6011	0.9053	−6174	0.9759	−4288
0.2967	−2648	0.5294	−4554								

[a] Mole fraction of CO_2. [b] Two-phase region.

where a_i and k are adjustable parameters, x_i is the liquid mole fraction of component i, and N is the number of adjustable parameters. The experimental data were also correlated using the PR EOS[21]

$$P = \frac{RT}{v - b} - \frac{a(T)}{v(v + b) + b(v - b)} \tag{2}$$

Table 3. Pure Component Critical Data and Acetric Factor ω in the Calculations Using the PR EOS

component	T_c/K ^{a}	P_c/MPa^a	ω^a
CO_2	304.12	7.374	0.225
DMC	557.00	4.800	0.336

[a] Poling et al.[22]

where P is the pressure, R is the gas constant, T is the temperature, v is the molar volume, a is the energy parameter, and b is the size parameter. In this study, the

Table 4. Determined Parameters and Deviations between Experimental and Calculated H^E for the System CO_2 (1) + DMC (2) Using Equations 1 and 5

parameter	5.0 MPa	5.5 MPa	6.0 MPa	6.5 MPa	7.0 MPa	7.5 MPa
			298.15 K One-Phase Region			
k	0.95127	0.96035	0.99099			
a_0/J·mol^{-1}	-2.3480×10^4	-2.2344×10^4	-2.0908×10^4			
a_1/J·mol^{-1}	9.4343×10^1	5.9540×10^2	1.8021×10^3			
a_2/J·mol^{-1}			1.9060×10^3			
$\Delta_1{}^a$/J·mol^{-1}	39	32	45			
$\Delta_2{}^b$/%	0.4	0.4	0.6			
			298.15 K Two-Phase Region			
A/J·mol^{-1}	-5.3718×10^4	-1.0066×10^5	-2.3103×10^5			
$\Delta_1{}^a$/J·mol^{-1}	98	73	489			
$\Delta_2{}^b$/%	1.1	0.8	6.2			
			298.15 K Overall			
$\Delta_1{}^a$/J·mol^{-1}	56	36	92			
$\Delta_2{}^b$/%	0.6	0.4	1.2			
			303.15 K One-Phase Region			
k	0.94030	0.94755	0.95900			
a_0/J·mol^{-1}	-2.3702×10^4	-2.2730×10^4	-2.1622×10^4			
a_1/J·mol^{-1}	3.8099×10^1	4.8624×10^2	8.2622×10^2			
$\Delta_1{}^a$/J·mol^{-1}	18	31	31			
$\Delta_2{}^b$/%	0.2	0.4	0.4			
			303.15 K Two-Phase Region			
A/J·mol^{-1}	-3.7542×10^4	-5.1453×10^4	-7.8816×10^4			
$\Delta_1{}^a$/J·mol^{-1}	119	102	52			
$\Delta_2{}^b$/%	1.4	1.2	0.6			
			303.15 K Overall			
$\Delta_1{}^a$/J·mol^{-1}	49	52	35			
$\Delta_2{}^b$/%	0.6	0.6	0.4			
			308.15 K One-Phase Region			
k	0.93428	0.93296	0.96977	0.95027	0.97490	0.92563
a_0/J·mol^{-1}	-2.4017×10^4	-2.3286×10^4	-2.2119×10^4	-2.0932×10^4	-1.9571×10^4	-1.7265×10^4
a_1/J·mol^{-1}	5.3606×10^2	4.6449×10^2	1.4340×10^3	1.0031×10^3	1.8796×10^3	1.1311×10^3
a_2/J·mol^{-1}			1.0723×10^3	9.1262×10^2	1.1575×10^3	-2.7034×10^3
a_3/J·mol^{-1}				-4.8868×10^2		-1.3452×10^3
a_4/J·mol^{-1}				-1.3058×10^3		1.6820×10^4
a_5/J·mol^{-1}						-1.0503×10^3
a_6/J·mol^{-1}						-2.1351×10^4
$\Delta_1{}^a$/J·mol^{-1}	14	26	18	24	21	40
$\Delta_2{}^b$/%	0.2	0.3	0.2	0.3	0.3	0.6
			308.15 K Two-Phase Region			
A/J·mol^{-1}	-2.8459×10^4	-3.5920×10^4	-4.7976×10^4	-6.9424×10^4	-1.0350×10^5	
$\Delta_1{}^a$/J·mol^{-1}	181	88	104	95	92	
$\Delta_2{}^b$/%	2.2	1.1	1.3	1.2	1.3	
			308.15 K Overall			
$\Delta_1{}^a$/J·mol^{-1}	92	42	44	35	31	40
$\Delta_2{}^b$/%	1.1	0.5	0.6	0.4	0.4	0.6

[a] $\Delta_1 = \{\sum_k |H^E_{\text{exptl}} - H^E_{\text{calcd}}|_k\}/\text{NDP}$. [b] $\Delta_2 = (100/\text{NDP})\sum_k |(H^E_{\text{exptl}} - H^E_{\text{calcd}})/H^E_{\text{exptl(max)}}|_k$, where $H^E_{\text{exptl(max)}}$ is the maximum experimental H^E data in a given data set.

following van der Waals one-fluid mixing rules were used for the mixture energy parameter a and the size parameter b

$$a = \sum_i \sum_j x_i x_j (a_{ii} a_{jj})^{0.5} (1 - k_{ij}) \tag{3}$$

$$b = \sum_i x_i b_i \tag{4}$$

where k_{ij} is a binary interaction parameter. Pure component parameters, necessary for calculating the a and b values of pure components of interest in this study, are shown in Table 3.

In this study, it was difficult to determine the end of the mole fraction of CO_2 that formed the two-phase region from the experimental results of H^E. Therefore, the end of the two-phase region was treated as $x_1 = 1$, and the linear section of the H^E values was expressed using the following equation

$$H^E/\text{J·mol}^{-1} = A(1 - x_1) \tag{5}$$

where A is a adjustable parameter.

Fitting parameters a_i and k in eq 1, k_{ij} in the PR EOS, and A_i in eq 5 were estimated so that the following objective function was minimized for each system by means of the Marquardt algorithm[23]

$$\text{OF} = \sum_{k=1}^{\text{NDP}} (H^E_{\text{exptl}} - H^E_{\text{calcd}})_k^2 \tag{6}$$

where NDP is the number of experimental data points and H^E_{exptl} and H^E_{calcd} are the experimental and calculated H^E values, respectively.

The estimated parameters of eqs 1, 3, and 5 and the deviations between the correlated and experimental H^E data are given in Tables 4 and 5. The value of N in eq 1

Table 5. Determined Parameters and Deviations between Experimental and Calculated H^E for the System CO_2 (1) + DMC (2) Using the PR EOS

parameter	5.0 MPa	5.5 MPa	6.0 MPa	6.5 MPa	7.0 MPa	7.5 MPa
298.15 K One-Phase Region: $k_{12} = -7.7236 \times 10^{-2}$						
$\Delta_1{}^a$/J·mol^{-1}	141	166	185			
$\Delta_2{}^b$/%	1.6	2.0	2.3			
298.15 K Overall Containing Two-Phase Region						
$\Delta_1{}^a$/J·mol^{-1}	129	156	217			
$\Delta_2{}^b$/%	1.4	1.8	2.7			
303.15 K One-Phase Region: $k_{12} = -8.5867 \times 10^{-2}$						
$\Delta_1{}^a$/J·mol^{-1}	121	133	176			
$\Delta_2{}^b$/%	1.4	1.6	2.2			
303.15 K Overall Containing Two-Phase Region						
$\Delta_1{}^a$/J·mol^{-1}	120	124	153			
$\Delta_2{}^b$/%	1.4	1.5	1.9			
308.15 K One-Phase Region: $k_{12} = -8.4216 \times 10^{-2}$						
$\Delta_1{}^a$/J·mol^{-1}	82	137	113	158	163	246
$\Delta_2{}^b$/%	1.0	1.7	1.4	2.0	2.3	4.0
308.15 K Overall Containing Two-Phase Region						
$\Delta_1{}^a$/J·mol^{-1}	128	125	110	148	153	246
$\Delta_2{}^b$/%	1.6	1.5	1.4	1.9	2.1	4.0

[a] $\Delta_1 = \{\Sigma_k |H^E_{\text{exptl}} - H^E_{\text{calcd}}|_k\}/\text{NDP}$. [b] $\Delta_2 = (100/\text{NDP})\Sigma_k|(H^E_{\text{exptl}} - H^E_{\text{calcd}})/H^E_{\text{exptl(max)}}|_k$, where $H^E_{\text{exptl(max)}}$ is the maximum experimental H^E data in a given data set.

Table 6. Solubility Limits from H^E for the System CO_2 (1) + DMC (2)

P/MPa	x_1	H^E/J·mol^{-1} (calcd)
	298.15 K	
5.0	0.8344	−8894
5.5	0.9170	−8353
6.0	0.9674	−7520
	303.15 K	
5.0	0.7726	−8537
5.5	0.8357	−8455
6.0	0.8970	−8120
	308.15 K	
5.0	0.7152	−8104
5.5	0.7710	−8227
6.0	0.8308	−8119
6.5	0.8893	−7686
7.0	0.9339	−6843

was changed at each temperature and pressure for the H^E data, considering the correlation accuracy in the polynomial expression model. With respect to the PR EOS, the binary parameter k_{12} was determined at each temperature independently of the pressure. It can be seen from Tables 4 and 5 that both models give reasonable correlated results at all temperatures and pressures in the one-phase region and that the results from the polynomial expression model are better than those from the PR EOS. The results correlated by the polynomial expression model are shown graphically in Figures 1−3.

Finally, we determined the carbon dioxide liquid composition in the vapor−liquid equilibrium of this mixture at temperatures and pressures where a two-phase region was formed. This liquid composition was obtained by combining eqs 1 and 5. The carbon dioxide liquid compositions determined are summarized in Table 6 and illustrated in Figures 1−3. In this study, these results were compared with the VLE data of this system predicted on the basis of the experimental H^E data in order to examine the consistency of the measurements in the separation region of gases and liquids. The VLE at (298.15, 303.15, and 308.15) K were calculated using the PR EOS with the binary parameter k_{12} from the correlation of H^E. The liquid compositions determined from the H^E data are compared with the predicted VLE data in Figure 4. As can be seen in Figure 4, the liquid compositions of carbon dioxide at each temperature and pressure are in relatively good agreement with the VLE data calculated from the H^E data. Therefore, it seems that appropriate H^E data are obtained over a wide range of concentrations that include the vapor−liquid equilibrium region.

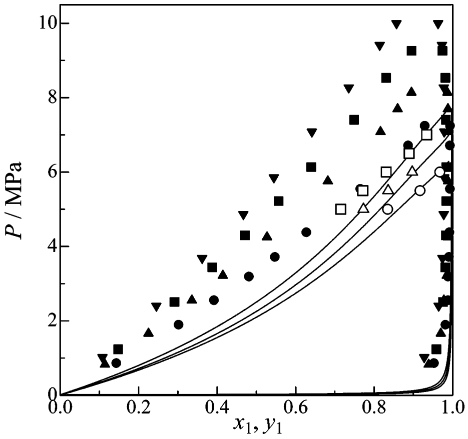

Figure 4. Comparison of the calculated solubility limit points from the experimental H^E data for the system CO_2 (1) + DMC (2) with the predicted VLE data on the basis of the experimental H^E. This work: ○, 298.15 K; △, 303.15 K; □, 308.15 K. −, Predicted VLE using the PR EOS with k_{12} determined from the H^E correlations. Literature VLE data: ●, 310.27 K; ▲, 320.36 K; ■, 330.30 K; ▼, 340.27 K.[17]

Conclusions

Excess molar enthalpies were determined for the CO_2 + DMC system over the entire composition range at temperatures from (298.15 to 308.15) K and pressures from (5.0 to 7.5) MPa. In this system, the experimental H^E data were exothermic for all compositions at all of the temperatures and pressures studied, with the exception of being slightly endothermic in the extremely carbon dioxide-rich region at 5.0 MPa at temperatures of (298.15 and 308.15) K. The maximum exothermic value of the H^E data was about 8.9 kJ·mol^{-1} at 298.15 K and 5.0 MPa. At all temperatures and pressures except 308.15 K and 7.5 MPa, a two-phase region, where H^E varies linearly with composition, was found in the CO_2-rich region. The experimental results were correlated with the polynomial expression model, the PR EOS, and the linear expression for the mole fraction of carbon dioxide in the two-phase region. The carbon dioxide liquid composition in the vapor−liquid equilibrium was also determined from the H^E data. These compositions were comparable with the VLE data predicted using the PR EOS with the parameter k_{12} obtained from the correlation of H^E. This shows that the experimentally determined H^E data in this study are reasonable over a wide range of compositions including the two-phase region. These experimental H^E data that exhibit a large heat effect should be useful for the design and development of energy-saving processes.

Literature Cited

(1) Christensen, J. J.; Christensen, S. P.; Schofield, R. S.; Faux, P. W.; Harding, P. R.; Izatt, R. M. The excess enthalpies of (carbon dioxide + pyridine) at 308.15, 358.15, and 413.15 K from 7.50 to 12.50 MPa. *J. Chem. Thermodyn.* **1984**, *16*, 249−255.

(2) Christensen, J. J.; Walker, T. A. C.; Schofield, R. S.; Faux, P. W.; Harding, P. R.; Izatt, R. M. The excess enthalpies of (carbon dioxide + hexane) at 308.15, 358.15, and 413.15 K from 7.50 to 12.50 MPa. *J. Chem. Thermodyn.* **1984**, *16*, 445−451.

(3) Christensen, J. J.; Cordray, D.; Izatt, R. M. The excess enthalpies of (carbon dioxide + decane) from 293.15 to 573.15 K at 12.50 MPa. *J. Chem. Thermodyn.* **1986**, *18*, 53−61.
(4) Christensen, J. J.; Cordray, D. R.; Oscarson, J. L.; Izatt, R. M. The excess enthalpies of four (carbon dioxide + an alkanol) mixtures from 308.15 to 573.15 K at 7.50 to 12.50 MPa. *J. Chem. Thermodyn.* **1988**, *20*, 867−875.
(5) Dai, W.; Ochi, K.; Kurihara, K.; Kojima, K.; Hongo, M. Measurement and Correlation of Excess Enthalpy for the System (CO_2 + CH_3OH) Containing Supercritical Carbon Dioxide. *Jpn. J. Thermophys. Prop.* **1998**, *12*, 64−69.
(6) Dai, W.; Kojima, K.; Ochi, K. Measurement and Correlation of Excess Molar Enthalpies of CO_2 + CH_3OH System in the Vicinity of Critical Point of Carbon Dioxide. *J. Chem. Eng. Data* **1999**, *44*, 161−164.
(7) Dai, W.; Kojima, K.; Ochi, K. Measurement and Correlation of Excess Molar Enthalpies of Carbon Dioxide + 2-Butanol and 2-Propanol System at the Temperatures 303.15 K and 308.15 K and at Pressures from 7.0 to 8.5 MPa. *J. Chem. Eng. Data* **2000**, *45*, 6−10.
(8) Ochi, K.; Dai, W.; Wada, Y.; Hayashi, H.; Kurihara, K.; Kojima, K. Measurement and Correlation of Excess Molar Enthalpies for the Systems Containing Supercritical Carbon Dioxide and Alcohols. *Fluid Phase Equilib.* **2002**, *194−197*, 919−928.
(9) Ono, Y. Catalysis in the Production and Reaction of Dimethyl Carbonate, an Environmentally Benign Building Block. *Appl. Catal., A* **1997**, *15*, 133−166.
(10) Tundo, P.; Selva, M. The Chemistry of Dimethyl Carbonate. *Acc. Chem. Res.* **2002**, *35*, 706−716.
(11) Tundo, P.; Anastas, P. *Green Chemistry: Challenging Perspectives*; Oxford University Press: Oxford, U.K., 2001.
(12) Fang, S.; Fujimoto, K. Direct Synthesis of Dimethyl Carbonate from Carbon Dioxide and Methanol Catalyzed by Base. *Appl. Catal., A* **1996**, *142*, L1−L3.
(13) Isaacs, N.; O'Sullivan, B.; Verhaelen, C. High-Pressure Routes to Dimethyl Carbonate from Superctirical Carbon Dioxide. *Tetrahedron* **1999**, *55*, 11949−11956.
(14) Sakakura, T.; Choi, J.; Saito, Y.; Sako, T. Synthesis of Dimethyl Carbonate from Carbon Dioxide: Catalysis and Mechanism. *Polyhedron* **2000**, *19*, 573−576.
(15) Chu, G.; Park, J.; Cheong, M. Synthesis of Dimethyl Carbonate from Carbon Dioxide over Polymer-Supported Iodide Catalysis. *Inorg. Chim. Acta* **2000**, *307*, 131−137.
(16) Camy, S.; Pic, J.-S.; Badens, E.; Conodret, J.-S. Fluid Phase Equilibria of the Reacting Mixture in the Dimethyl Carbonate Synthesis from Supercritical CO_2. *J. Supercrit. Fluids* **2003**, *25*, 19−32.
(17) Im, J.; Kim, M.; Lee, J.; Kim, H. Vapor−Liquid Equilibria of Binary Carbon Dioxide + Alkyl Carbonate Mixture Systems. *J. Chem. Eng. Data* **2004**, *49*, 243−245.
(18) Nagashima, A.; Yoshii, S.; Matsuda, H.; Ochi K. Measurement and Correlation of Excess Molar Enthalpies for Ethylene Glycol + Alkanol Systems at the Temperatures (298.15, 308.15, and 323.15) K. *J. Chem. Eng. Data* **2004**, *49*, 286−290.
(19) Mallard W. G., Linstrom, P. J. *NIST Chemistry WebBook*; NIST Standard Reference Database Number 69; National Institute of Standards and Technology: Gaithersburg, MD, 2003.
(20) Lugo. L.; Comunas, M. J. P.; Lopez, E. R.; Fernandez, J.; (p, V_m, T, x) Measurements of Dimethyl Carbonate + Octane Binary Mixtures I. Experimental Results, Isothermal Compressibilities, Isobaric Expansivities and Internal Pressures. *Fluid Phase Equilib.* **2001**, *186*, 235−255.
(21) Peng, D.; Robinson, D. B. A New Two-Constant Equation of State. *Ind. Eng. Chem. Fundam.* **1976**, *15*, 59−64.
(22) Poling, B. E.; Prausnitz, J. M.; O'Connel, J. P. *The Properties of Gases and Liquids*, 5th ed.; McGraw-Hill: New York, 2001.
(23) Marquardt, D. W. An Algorithm for Least-Squares Estimation of Nonlinear Parameters. *J. Soc. Ind. Appl. Math.* **1963**, *11*, 431−441.

Received for review March 7, 2005. Accepted April 20, 2005.

JE050089U